BCS-BEC crossover in nuclear matter with the relativistic Hartree-Bogoliubov theory

Ting Ting Sun (孙亭亭),[1] Bao Yuan Sun (孙保元),[2,3,1] and Jie Meng (孟杰)[1,4,5,*]

[1]*School of Physics and State Key Laboratory of Nuclear Physics and Technology, Peking University,
100871 Beijing, People's Republic of China*
[2]*School of Nuclear Science and Technology, Lanzhou University, 730000 Lanzhou, People's Republic of China*
[3]*Research Center for Nuclear Physics (RCNP), Osaka University, Ibaraki, 567-0047 Osaka, Japan*
[4]*School of Physics and Nuclear Energy Engineering, Beihang University, 100191 Beijing, People's Republic of China*
[5]*Department of Physics, University of Stellenbosch, 7602 Stellenbosch, South Africa*

Based on the relativistic Hartree-Bogoliubov theory, the influence of the pairing interaction strength on the dineutron correlations and the crossover from superfluidity of neutron Cooper pairs in the $^1S_0$ channel to Bose-Einstein condensation of dineutron pairs is systematically investigated in the nuclear matter. The bare nucleon-nucleon interaction Bonn-B is taken in the particle-particle channel with an effective factor to simulate the medium effects and take into account the possible ambiguity of pairing force, and the effective interaction PK1 is used in the particle-hole channel. If the effective factor is larger than 1.10, a dineutron Bose-Einstein condensation (BEC) state appears in the low-density limit, and if it is smaller than 0.85, the neutron Cooper pairs are found totally in the weak coupling Bardeen-Cooper-Schrieffer (BCS) region. The reference values of several characteristic quantities which characterize the BCS-BEC crossover are obtained, respectively, from the dimensionless parameter $1/(k_{\mathrm{Fn}}a)$ with a the scattering length and k_{Fn} the neutron Fermi momentum, the zero-momentum transfer density correlation function $D(0)$, and the effective chemical potential ν_{n}.

I. INTRODUCTION

The BCS-BEC crossover, which is described as the evolution of the pairing phenomenon from the weakly coupled Bardeen-Cooper-Schrieffer (BCS) type to the strongly correlated Bose-Einstein condensation (BEC) state with increasing pairing interaction, is one of the important issues in the study of the pairing correlations in Fermion systems. The transition from BCS to BEC was investigated theoretically in several domains of physics, such as in excitonic semiconductors [1], superconductors [2], and attractive Fermi gases [3]. Although BCS and BEC are physically two quite different limits, it was found that the evolution between them is smooth and continuous [2–4].

Since the strength of interatomic interaction can be controlled via a magnetically driven Feshbach resonance, ultracold Fermi atomic gases provide a special laboratory for studying strongly correlated Fermion systems. Recently, the BCS-BEC crossover phenomenon has been experimentally realized in ultracold quantum atomic gas [5–7].

In nuclear physics, however, the BCS-BEC crossover phenomenon is still a challenging topic because of the impossibility to control the nuclear pairing force directly. Indirectly, one can change the strength of pairing interaction in nuclear matter by altering density or temperature. As a result, density and temperature are treated as important parameters in the study of nuclear pairing correlations.

For the neutron-proton pairing, the BCS-BEC crossover has been investigated in the $^3S_1$-$^3D_1$ channel, in which the strong spatial correlation and the BEC of the deuterons may occur at low densities [8–13].

For the neutron-neutron pairing, the correlation is expected to be significant in low-density nuclear matter as well. It is well known that the bare neutron-neutron interaction in the $^1S_0$ channel leads to a virtual state around zero energy characterized by a large negative scattering length $a \approx -18.5 \pm 0.4\,\mathrm{fm}$ [14], implying a very strong attraction between two neutrons in the spin singlet state. Furthermore, theoretical predictions suggest that around one-tenth of the normal nuclear density ρ_0, the $^1S_0$ pairing gap may take a considerably larger value than that around ρ_0 [15–17]. In addition, the strong dineutron correlations are also supported by the enhancement of two-neutron transfer cross sections in several heavy nuclei [18]. In the weakly bound neutron-rich nuclei, dineutron correlations are enhanced due to the couplings with the continuum and play an important role for unstable nucleus and the formation of nuclear halo [19–21]. Recently, dineutron emission in ^{16}Be was observed for the first time, indicating the structure of dineutron clusters inside neutron-rich nuclei [22].

The progress in both theoretical and experimental investigations on dineutron correlations in weakly bound nuclei has stimulated lots of interest in searching for possible BCS-BEC crossover of neutron pairing. The influences on dineutron correlations by the Skyrme-type density dependent force and the finite-range Gogny force are discussed in Ref. [21]. In nuclear matter, the study of the BCS-BEC crossover phenomenon was mainly performed by using the finite-range Gogny interaction and the zero-range contact interaction [23–26]. It has been found that the dineutron correlations get stronger as density decreases, and BCS-BEC

*mengj@pku.edu.cn

crossover could occur at low densities. Besides, based on the bare force given by a superposition of three Gaussian functions [23] or the bare nucleon-nucleon interaction Bonn potential [27], the BCS-BEC crossover in the nuclear matter has also been investigated. It was shown that the spatial structure of the wave function for the neutron Cooper pairs evolves from BCS-type to BEC-type as density decreases. From several characteristic quantities, such as the effective chemical potential, the quasiparticle excitation spectrum and the density correlation function, there is no evidence for the BEC state of dineutron pairs at any density. However, it was argued that a Bose dineutron gas may be found in the low-density limit in quasi-two-dimensional neutron systems as long as the slab is thin enough [28]. Recently, the study on the BCS-BEC crossover phenomenon has been extended to finite temperature [29]. The thermodynamic signal from the temperature dependence of specific heat suggests that BCS-BEC crossover has been found in the low-density region. In finite nuclei, the coexistence of BCS- and BEC-like spatial structures of dineutron wave functions has also been revealed in the halo nucleus ^{11}Li [30]. From the dineutron wave function, a strong correlation between the valence neutrons appears on the surface of the nucleus.

For most investigations on dineutron correlations, for convenience, the phenomenological effective nuclear forces are used in the particle-particle (pp) channel. The effective interactions in the relativistic mean-field (RMF) theory are also used in the pp channel [31–33]. However, one has to introduce an effective factor for this kind of pairing interaction in order to obtain reasonable values for the gap parameter [33]. In fact, details of the effective nucleon-nucleon interaction in nuclear matter and finite nuclei are as yet not completely clarified, since most of the experimental data are not very sensitive to their details. It is generally believed that the bare nucleon-nucleon interaction should be corrected by the medium polarization effects (also referred to as the screening effects) in extracting the effective interactions in pp channel at various densities [34]. Therefore, it is of great interest to study the behavior of dineutron correlations and the BCS-BEC crossover phenomenon with different strengths of the pairing interaction.

As the RMF theory has achieved lots of success in the descriptions of both nuclear matter and finite nuclei near or far from the stability line [35–37], following a previous investigation [27], the influence of the strength of pairing interaction on dineutron correlations in the $^1S_0$ channel will be studied with the relativistic Hartree-Bogoliubov (RHB) theory in nuclear matter in this work. The bare nucleon-nucleon interaction, i.e., the relativistic Bonn potential [38], will be adopted in the pp channel with an effective factor to simulate the medium polarization effects and take into account the possible ambiguity of pairing force [34], and the relativistic mean-field model is used in the particle-hole (ph) channel. The pairing strength marking the crossover from the strong correlated BEC state to the weakly correlated BCS state will be discussed. Section II briefly introduces the formulism of the RHB theory for nuclear matter. The results are given and discussed in Sec. III and finally the work is summarized in Sec. IV.

II. THEORETICAL FRAMEWORK

The RMF model with nonlinear σ- and ω-meson self-coupling is employed in the ph channel to describe the bulk properties of the nuclear matter [35–37]. For the static and uniform infinite nuclear matter, the Coulomb field is neglected and the space-like components as well as the differential of the time-like components of the meson fields vanish.

In the RHB theory, the meson fields are treated dynamically beyond the mean-field approximation to provide the pairing field via the anomalous Green's functions, which gives a uniform description for the mean field and the pairing field [31]. In the case of infinite nuclear matter, the RHB equation is reduced to the usual BCS equation. The BCS ground state is defined as

$$|\text{BCS}\rangle = \prod_{k>0}(u_k + v_k\hat{a}^\dagger_{k\uparrow}\hat{a}^\dagger_{-k\downarrow})|-\rangle, \quad (1)$$

where u_k and v_k represent the BCS variational parameters, and $\hat{a}^\dagger_{k\uparrow}$ ($\hat{a}^\dagger_{-k\downarrow}$) are creation operators of a particle with momentum $\boldsymbol{k}$ ($-\boldsymbol{k}$) and spin $\uparrow$ ($\downarrow$) on top of the vacuum $|-\rangle$ [39].

For the $^1S_0$ channel, the pairing gap function $\Delta(p)$ satisfies

$$\Delta(p) = -\frac{1}{(2\pi)^3}\int \lambda \cdot v_{pp}(\boldsymbol{k}, \boldsymbol{p})\frac{\Delta(k)}{2E_k}d\boldsymbol{k}, \quad (2)$$

where $v_{pp}(\boldsymbol{k}, \boldsymbol{p})$ is the matrix element of nucleon-nucleon interaction in the momentum space. Here an effective pairing interaction factor λ is introduced to control the pairing interaction strength. The quasiparticle energy E_k can be written as

$$E_k = \sqrt{(\varepsilon_k - \mu)^2 + \Delta(k)^2}, \quad (3)$$

with the single-particle energy ε_k and the chemical potential μ. The corresponding normal and anomalous density distribution functions are given in the following forms:

$$\rho_k = \frac{1}{2}\left[1 - \frac{\varepsilon_k - \mu}{E_k}\right], \quad \kappa_k = \frac{\Delta(k)}{2E_k}. \quad (4)$$

The single-particle energy ε_k follows from the RMF theory:

$$\varepsilon_k = \Sigma_0 + \sqrt{k^2 + M^{*2}}, \quad (5)$$

where Σ_0 is the vector potential, Σ_S the scalar potential, M the nucleon mass, and $M^* = M + \Sigma_S$ the effective mass,

$$\Sigma_S = g_\sigma\sigma, \quad \Sigma_0 = g_\omega\omega_0 + g_\rho\tau_3\rho_{0,3}, \quad (6)$$

with g_σ, g_ω, and g_ρ the meson-nucleon coupling constants of the respective meson fields σ, ω_0, and $\rho_{0,3}$, and τ_3 the third component of the nucleon isospin.

With the mean-field approximation, the meson fields are replaced by their mean values, and could be solved from the corresponding equations of motion with the given nucleon densities,

$$m_\sigma^2\sigma = -g_\sigma\rho_s - g_2\sigma^2 - g_3\sigma^3, \quad (7)$$

$$m_\omega^2\omega_0 = g_\omega\rho_b - c_3\omega_0^3, \quad (8)$$

$$m_\rho^2\rho_{0,3} = g_\rho\rho_{b,3}, \quad (9)$$

where ρ_s, ρ_b, and $\rho_{b,3}$ are, respectively, the scalar density, vector density, and isospin vector density,

$$\rho_s = \frac{1}{\pi^2} \sum_{i=n,p} \int_0^\infty \frac{M_i^*}{\sqrt{k^2 + M_i^{*2}}} \rho_{k,i} k^2 dk, \qquad (10)$$

$$\rho_b = \rho_n + \rho_p = \frac{1}{\pi^2} \sum_{i=n,p} \int_0^\infty \rho_{k,i} k^2 dk, \qquad (11)$$

$$\rho_{b,3} = \frac{1}{\pi^2} \sum_{i=n,p} \int_0^\infty \tau_3 \rho_{k,i} k^2 dk. \qquad (12)$$

The nucleon Fermi momentum $k_{\text{F}i}(i = n, p)$ is defined by the nucleon densities ρ_i with $\rho_i \equiv k_{\text{F}i}^3/3\pi^2$. Therefore, for nuclear matter with given baryonic density ρ_b and isospin asymmetry $\zeta = (\rho_n - \rho_p)/\rho_b$, the above equations can be solved by a self-consistent iteration method with no-sea approximation. Accordingly, the chemical potential μ is obtained via solving Eqs. (2), (4), and (11) by the self-consistent iteration.

The relativistic Bonn potential is used in the pp channel, which has a proper momentum behavior determined by the scattering data up to high energies [38]. It is defined as the sum of one-boson-exchange (OBE) potential of the six bosons $\phi = \sigma, \omega, \pi, \rho, \eta, \delta$. The vector meson ρ includes the vector coupling channel ρ^V, the tensor coupling channel ρ^T, and the vector-tensor coupling channel ρ^{VT}, and the pseudoscalar mesons π and η include the pseudoscalar coupling channel π^{PV} and η^{PV}, respectively.

The matrix element $v_{pp}(\boldsymbol{k}, \boldsymbol{p})$ is

$$v_{pp}(\boldsymbol{k}, \boldsymbol{p}) = \sum_\phi \frac{\eta_\phi}{2\varepsilon_k^* \varepsilon_p^*} A_\phi(\boldsymbol{k}, \boldsymbol{p}) D_\phi(\boldsymbol{q}^2) F_\phi^2(\boldsymbol{q}^2), \qquad (13)$$

where ε_k^* is the effective single-particle energy

$$\varepsilon_k^* = \sqrt{k^2 + M^{*2}}. \qquad (14)$$

$D_\phi(\boldsymbol{q}^2)$ is a meson propagator with the momentum transfer $\boldsymbol{q} = \boldsymbol{k} - \boldsymbol{p}$, and $F_\phi(\boldsymbol{q}^2)$ is a form factor in order to get the reasonable value for the pairing gap,

$$D_\phi(\boldsymbol{q}^2) = \frac{1}{\boldsymbol{q}^2 + m_\phi^2}, \quad F_\phi(\boldsymbol{q}^2) = \frac{\Lambda_\phi^2 - m_\phi^2}{\boldsymbol{q}^2 + \Lambda_\phi^2}, \qquad (15)$$

with the meson mass m_ϕ and the cutoff parameter Λ_ϕ. The vertex functions of the OBE potential η_ϕ and $A_\phi(\boldsymbol{k}, \boldsymbol{p})$ are listed in Table I. For the $^1S_0$ pairing channel, the matrix element $v_{pp}(k, p)$ is related to $v_{pp}(\boldsymbol{k}, \boldsymbol{p})$ by the integral,

$$v_{pp}(k, p) = \int_0^\pi v_{pp}(\boldsymbol{k}, \boldsymbol{p}) \sin\theta d\theta, \qquad (16)$$

where θ is the angle between the vectors $\boldsymbol{k}$ and $\boldsymbol{p}$.

In the following calculations, Bonn-B potential [38] will be adopted for $v_{pp}(\boldsymbol{k}, \boldsymbol{p})$ and the effective interaction PK1 [41] of the relativistic mean-field theory is used in the ph channel.

III. RESULTS AND DISCUSSION

In the following discussion, the pure neutron matter will be mainly selected to clarify the physics. To simulate the medium polarization effects and take into account the possible ambiguity of pairing force [34], the effective pairing interaction

TABLE I. The vertex functions η_ϕ and $A_\phi(\boldsymbol{k}, \boldsymbol{p})$ of the OBE potential in the relativistic Bonn-B potential with the corresponding parameters g_σ^B, g_δ^B, g_ω^B, g_ρ^B, f_ρ^B, f_π^B, and f_η^B. The general expression could be found in Ref. [40]. See the text for details.

mesons	ϕ	η_ϕ	$A_\phi(\boldsymbol{k}, \boldsymbol{p})$
scalar	σ	$-(g_\sigma^B)^2$	$M^{*2} + \varepsilon_k^* \varepsilon_p^* - \boldsymbol{k} \cdot \boldsymbol{p}$
	δ	$-(g_\delta^B)^2$	$M^{*2} + \varepsilon_k^* \varepsilon_p^* - \boldsymbol{k} \cdot \boldsymbol{p}$
vector	ω	$(g_\omega^B)^2$	$2(2\varepsilon_k^* \varepsilon_p^* - M^{*2})$
	ρ^V	$(g_\rho^B)^2$	$2(2\varepsilon_k^* \varepsilon_p^* - M^{*2})$
	ρ^T	$(f_\rho^B/2M)^2$	$(M^{*2} + 3\varepsilon_k^* \varepsilon_p^* + \boldsymbol{k} \cdot \boldsymbol{p})\boldsymbol{q}^2$
	ρ^{VT}	$(f_\rho^B g_\rho^B/M)M^*$	$\boldsymbol{q}^2$
pseudoscalar	π^{PV}	$(f_\pi^B/m_\pi)^2$	$(M^{*2} + \varepsilon_k^* \varepsilon_p^* + \boldsymbol{k} \cdot \boldsymbol{p})\boldsymbol{q}^2$
	η^{PV}	$(f_\eta^B/m_\eta)^2$	$(M^{*2} + \varepsilon_k^* \varepsilon_p^* + \boldsymbol{k} \cdot \boldsymbol{p})\boldsymbol{q}^2$

factor λ varying from 0.8 to 1.4 is taken in the calculations. When the pairing gaps at the Fermi surface, $\Delta_{\text{Fn}} \equiv \Delta(k_{\text{Fn}})$, are plotted as a function of the Fermi momentum k_{Fn} for different effective factor λ, a maximum $\Delta(k_{\text{Fn}})$ always appears around $k_{\text{Fn}} = 0.8$ fm^{-1} but changes from about 1.4 MeV for $\lambda = 0.8$ to about 6.5 MeV for $\lambda = 1.4$, and is 3.1 MeV for $\lambda = 1.0$, i.e., the relativistic Bonn-B potential.

For dineutron correlations in the low density region, the scattering length a in the $^1S_0$ channel, which is defined in terms of the T matrix for the scattering in the free space, is an important physical quantity. According to the definition, the negative value of the scattering length a indicates an unbound state of neutron Cooper pairs while the positive value represents a bound state. It has been proposed to define the boundaries of the BCS-BEC crossover using a regularized gap equation approach [2,23,42,43], which is related with the scattering length a. This approach is generically applied to dilute systems, where the interaction matrix elements $v_{pp}(\boldsymbol{k}, \boldsymbol{p})$ can be approximately treated as constant v_0. Using the zero-energy T matrix, the relation between the scattering length a in the $^1S_0$ channel and the constant interaction v_0 can be obtained as

$$\frac{M}{4\pi\hbar^2 a} = \frac{1}{v_0} + \frac{1}{(2\pi)^3} \int d\boldsymbol{k} \frac{1}{2e(k)}, \qquad (17)$$

where $e(k)$ is the neutron kinetic energy,

$$e(k) = \sqrt{k^2 + M^{*2}} - M^*. \qquad (18)$$

The pairing gap equation (2) becomes

$$1 = -\frac{1}{(2\pi)^3} \int v_0 \cdot \frac{1}{2E_k} d\boldsymbol{k}. \qquad (19)$$

From Eqs. (17) and (19), the regularized gap equation is written as

$$\frac{M}{4\pi\hbar^2 a} = -\frac{1}{2(2\pi)^3} \int d\boldsymbol{k} \left[\frac{1}{E_k} - \frac{1}{e(k)}\right]. \qquad (20)$$

Here instead of fixing the scattering length a from its physical value, it is treated as a variable calculated by Eq. (20) for different densities similarly as in Ref. [23]. The quasiparticle energy E_k and the neutron kinetic energy $e(k)$ in Eq. (20) are calculated by the momentum dependent pairing gap $\Delta(k)$
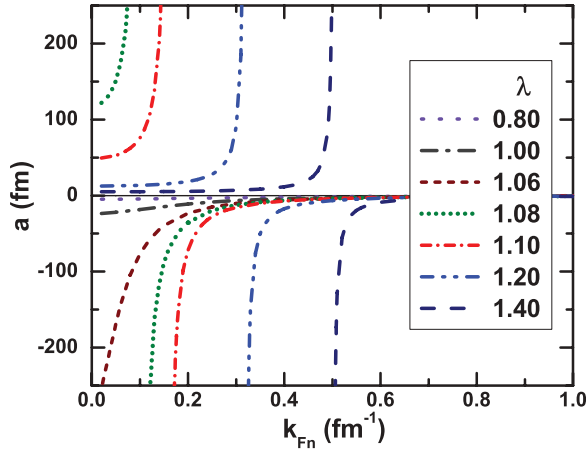
FIG. 1. (Color online) The neutron-neutron scattering length a in the $^1S_0$ channel as a function of the neutron Fermi momentum k_{Fn} for different effective pairing interaction factors λ in the pure neutron matter.
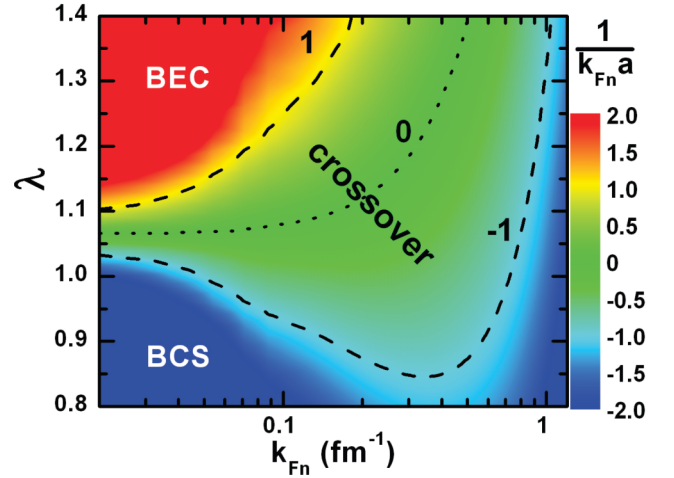

FIG. 2. (Color online) A contour plot for the dimensionless parameter $1/(k_{Fn}a)$ as a function of the neutron Fermi momentum k_{Fn} and the effective factor λ of pairing interaction in the pure neutron matter. The boundaries characterizing the BCS-BEC crossover $[1/(k_{Fn}a) = \pm 1]$ are denoted by the two dashed lines, while the unitarity limit between BCS and BEC regime $[1/(k_{Fn}a) = 0]$ is shown by the dotted line.

and the effective mass M^*, which are obtained from the self-consistent RHB theory with Bonn potential for the pairing force. This is different from the regularized contact interaction model [23], where constant pairing gap is used. However, the difference should be small in the low-density limit and comparable results are expected.

In Fig. 1, the neutron-neutron scattering length a in the $^1S_0$ channel is shown as a function of the neutron Fermi momentum k_{Fn} for different effective pairing interaction factors λ in the pure neutron matter. When $\lambda \leqslant 1.06$, only negative branch of the scattering length appears and the scattering length approaches zero at high densities, suggesting no bound state for neutron Cooper pairs. However, when $\lambda \geqslant 1.08$, the positive branch of the scattering length becomes available at the dilute density, which implies the occurrence of a possible dineutron bound state. For a given effective pairing interaction factor of $\lambda \geqslant 1.08$, with the increasing density, the scattering length starts from positive value and then diverges to positive infinity, and after crossing the Feshbach resonance, it reemerges from negative infinity. With increasing λ, the Feshbach resonance is shifted to higher density.

From the regularized gap equation (20), it was shown [23,43,44] that the properties of pairing correlations can be uniquely controlled by a dimensionless parameter $1/(k_{Fn}a)$ which can give the evolution from BCS to BEC. The dimensionless parameter $1/(k_{Fn}a) \ll -1$ corresponds to the weak coupling BCS regime, while $1/(k_{Fn}a) \gg 1$ is related to the strong correlated BEC regime. From weak coupling to strong attraction, the parameter $1/(k_{Fn}a)$ evolves smoothly from negative to positive. The boundaries characterizing the BCS-BEC crossover can be approximately determined by $1/(k_{Fn}a) = \pm 1$ [42,43,45]. The unitarity limit is defined as $1/(k_{Fn}a) = 0$, which is the midpoint of the BCS-BEC crossover.

In Fig. 2, a contour plot for the dimensionless parameter $1/(k_{Fn}a)$ of the neutron Cooper pairs is shown, as a function of the neutron Fermi momentum k_{Fn} and the effective pairing interaction factor λ in the pure neutron matter. The boundaries

of the BCS-BEC crossover $(1/(k_{Fn}a) = \pm 1)$ are denoted by the dashed lines, while the unitarity limit $(1/(k_{Fn}a) = 0)$ is shown by the dotted line. Distinct features of dineutron correlations are revealed for different pairing strengths.

At low density region with $k_{Fn} \lesssim 0.2$ fm^{-1}, the neutron Cooper pairs evolve continuously with the pairing strength from weak coupling BCS state to strong correlated BEC state. The effective factor λ corresponding to $1/(k_{Fn}a) = 1$ which characterizes the BEC boundary starts around $\lambda = 1.10$ in the low-density limit and increases with the density. The effective factor λ corresponding to $1/(k_{Fn}a) = 0$ which characterizes the unitarity limit starts around 1.07 in the low-density limit and increases with the density monotonically. The effective factor λ corresponding to $1/(k_{Fn}a) = -1$ which characterizes the BCS boundary starts around $\lambda = 1.03$ in the low-density limit, decreases with the density to a minimum $\lambda \sim 0.85$ at $k_{Fn} \sim 0.35$ fm^{-1}, then increases sharply.

Besides the dimensionless parameter $1/(k_{Fn}a)$, the density correlation function $D(q)$ [25,46], which describes the difference between the mean field and the pairing field, is also a useful quantity to study the dependence of dineutron correlations on the strength of pairing force. This measure can give the transition points from BCS state to BEC state but not the BCS-BEC crossover region. At zero-momentum transfer, i.e., $q = 0$, the density correlation function $D(q = 0)$ is reduced as

$$D(0) = \frac{1}{\pi^2 \rho_n} \int_0^\infty \left(\kappa_k^2 - \rho_k^2 \right) k^2 dk, \qquad (21)$$

where κ_k and ρ_k are from Eq. (4). The sign change of $D(0)$ has been considered as a criterion of the BCS-BEC crossover [25,46], i.e., $D(0) < 0$ means a BCS-type pairing and $D(0) > 0$ represents a dineutron BEC state.

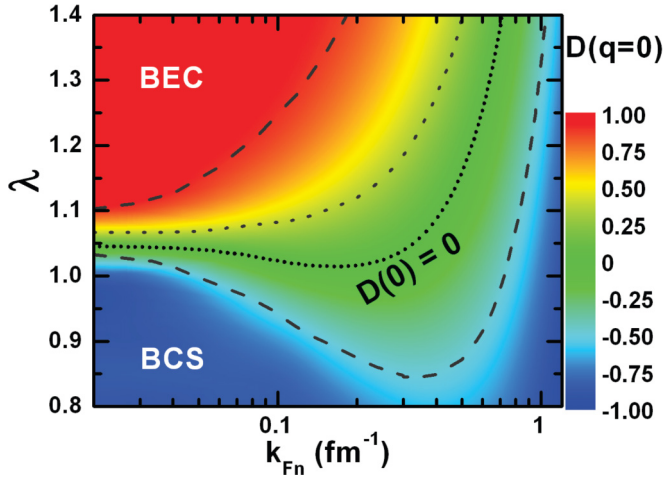In Fig. 3, the density correlation function at zero-momentum transfer $D(0)$ of the neutron Cooper pairs is

FIG. 3. (Color online) A contour plot for the density correlation function at zero-momentum transfer $D(0)$ as a function of the neutron Fermi momentum k_{Fn} and the effective factor λ of pairing interaction in the pure neutron matter. The boundary where $D(0) = 0$ is denoted by the short dotted line. For comparison, the two dashed lines characterizing the BCS-BEC crossover and the dotted line characterizing the unitarity limit between BCS and BEC regime in Fig. 2 are plotted as well.

FIG. 4. (Color online) A contour plot for the effective neutron chemical potential ν_n as a function of the neutron Fermi momentum k_{Fn} and the effective factor λ of pairing interaction in the pure neutron matter. The boundary of $\nu_n = 0$ is denoted by the short dotted line. For comparison, the two dashed lines characterizing the BCS-BEC crossover and the dotted line characterizing the unitarity limit between BCS and BEC regime in Fig. 2 are plotted as well.

shown as a function of the neutron Fermi momentum k_{Fn} and the effective pairing interaction factor λ for the pure neutron matter. The critical line $D(0) = 0$ is denoted by the short dotted line in comparison with the reference lines of $1/(k_{Fn}a) = \pm 1, 0$ obtained from Fig. 2.

In Fig. 3, it is revealed that the density correlation function $D(0)$ has a similar pattern as the dimensionless parameter $1/(k_{Fn}a)$. The effective factor λ corresponding to $D(0) = 0$ which characterizes the transition from BCS state to BEC state starts around $\lambda = 1.05$ in the low-density limit, decreases with the density to a minimum $\lambda \sim 1.02$ at $k_{Fn} \sim 0.20\,\text{fm}^{-1}$, then increases rapidly with the density. For $\lambda = 1.0$, the results show that no dineutron BEC state could occur, which agrees with previous results [27]. By taking the density correlation function $D(0) = 0$ as a measure, the effective factor λ characterizing the transition from BCS state to BEC state is smaller than the case by taking the unitarity limit $1/(k_{Fn}a) = 0$ as a measure.

In the case of the RMF theory, it has been proved that the neutron pair wave function in momentum space $\Psi_{pair}(k)$, i.e., the anomalous density κ_k in Eq. (4), satisfies a Schrödinger-like equation which is expressed as [27]

$$2e(k)\Psi_{pair}(k) + \frac{1 - 2\rho_k}{4\pi^2}\int_0^\infty \lambda \cdot v_{pp}(k, p)p^2 dp\,\Psi_{pair}(p)$$
$$= 2\nu_n\Psi_{pair}(k), \qquad (22)$$

with the corresponding energy eigenvalue $2\nu_n$, where ν_n is the effective neutron chemical potential obtained by deducting the momentum independent part from the chemical potential μ_n,

$$\nu_n = \mu_n - \Sigma_0 - M^*. \qquad (23)$$

In the limit of zero density, the effective chemical potential ν_n behaves as half binding energy of the Cooper pair [3]. For the evolution from the weak coupling BCS regime to the strongly
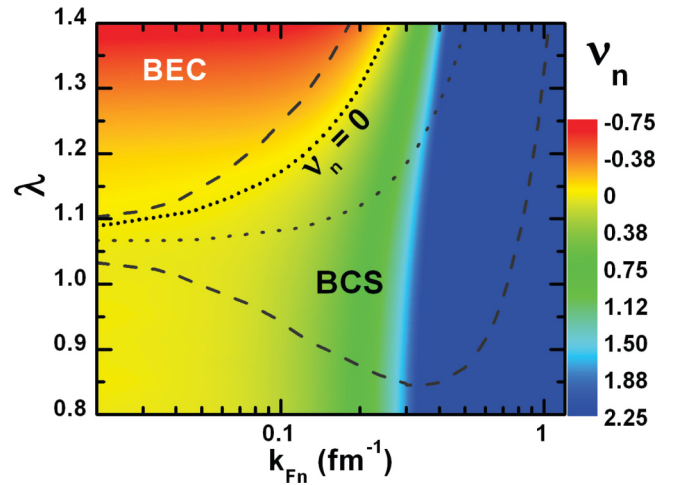
correlated BEC regime, the effective chemical potential ν_n is supposed to change from positive to negative.

In Fig. 4, a contour plot for the effective chemical potential ν_n of the neutron Cooper pair is shown as a function of k_{Fn} and λ in the pure neutron matter. The short dotted line denotes $\nu_n = 0$ in comparison with the dimensionless parameter $1/(k_{Fn}a) = \pm 1, 0$ extracted from Fig. 2.

The effective factor λ corresponding to $\nu_n = 0$ which characterizes the transition from BCS state to BEC state starts around $\lambda = 1.09$ in the low-density limit, then increases monotonically with the density. For $\lambda = 1.0$, there is no evidence for the BEC state of neutron pairs at any density, similarly as the case by taking density correlation function $D(0) = 0$ as a measure. By taking the effective chemical potential $\nu_n = 0$ as a measure, the effective factor λ characterizing the transition from BCS state to BEC state is larger than the case by taking the unitarity limit $1/(k_{Fn}a) = 0$ as a measure.

Combining the conclusions mentioned above, it can be summarized that a dineutron BEC state will appear in the low-density limit for $\lambda \geqslant 1.10$ and there is only a weak coupling BCS state for $\lambda \lesssim 0.85$. For $\lambda = 1.10$, the maximum pairing gap at the Fermi surface Δ_{Fn} is 4.12 MeV around the density $k_{Fn} = 0.8\,\text{fm}^{-1}$, and for $\lambda = 0.85$, it is 1.78 MeV.

For symmetric nuclear matter, recent studies have claimed that a dineutron BEC state can be formed at $k_{Fn} \sim 0.2\,\text{fm}^{-1}$ after considering the medium polarization effects [24,25]. In order to examine the above conclusion, similar investigation as the pure neutron matter for the symmetric nuclear matter has been done.

For symmetric nuclear matter, by taking the dimensionless parameter $1/(k_{Fn}a)$ as a measure, a dineutron BEC state will occur in the low-density limit for $\lambda \geqslant 1.10$ and neutron Cooper pairs are totally in the BCS state for $\lambda \lesssim 0.85$. By taking the density correlation function with zero-momentum transfer

TABLE II. Reference values of $P(d_n)$, ξ_{rms}/d_n, Δ_{Fn}/e_{Fn}, and ν_n/e_{Fn} characterizing the BCS-BEC crossover in the pure neutron matter (symmetric nuclear matter) respectively for the dimensionless parameter $1/(k_{Fn}a) = 0, \pm1$, the zero-momentum transfer density correlation function $D(0) = 0$, and the effective chemical potential $\nu_n = 0$ with effective pairing force factor $\lambda = 1.0, 1.1, 1.2$. For comparison, the results obtained for nuclear matter in the regularized contact interaction model [23,43] are also shown.

	λ	$1/(k_{Fn}a)$			$D(0)$	ν_n
		-1	0	$+1$	0	0
$P(d_n)$	1.0	0.82 (0.81)				
	1.1	0.82 (0.81)	0.99 (1.00)		0.95 (0.95)	
	1.2	0.82 (0.81)	0.99 (0.99)	1.00 (1.00)	0.96 (0.96)	1.00(1.00)
	[23]	0.81	0.99	1.00		
ξ_{rms}/d_n	1.0	0.98 (1.00)				
	1.1	0.98 (1.03)	0.35 (0.35)		0.52 (0.51)	
	1.2	0.98 (1.04)	0.38 (0.38)	0.19 (0.21)	0.52 (0.51)	0.26 (0.25)
	[23]	1.10	0.36	0.19		
Δ_{Fn}/e_{Fn}	1.0	0.25 (0.25)				
	1.1	0.26 (0.27)	0.74 (0.78)		0.56 (0.55)	
	1.2	0.28 (0.26)	0.83 (0.82)	1.52 (1.50)	0.59 (0.59)	1.20 (1.21)
	[23]	0.21	0.69	1.33		
ν_n/e_{Fn}	1.0	0.99 (0.98)				
	1.1	0.98 (0.98)	0.61 (0.61)		0.85 (0.84)	
	1.2	0.99 (0.99)	0.64 (0.63)	-0.84 (-0.87)	0.85 (0.85)	-0.01 (-0.01)
	[43]	0.97	0.60	-0.77		

$D(0)$ as a measure, the dineutron BEC state will appear in the low-density limit for $\lambda \gtrsim 1.05$. The minimum effective factor λ corresponding to $D(0) = 0$ is around 1.01 with the neutron Fermi momentum $k_{Fn} \sim 0.2 \, \text{fm}^{-1}$. By taking the effective chemical potential $\nu_n = 0$ as a measure, the effective factor λ characterizing the transition from BCS state to BEC state is larger than the case by taking the density correlation function $D(0) = 0$ as a measure and the dineutron BEC state may occur in the low-density limit for $\lambda \gtrsim 1.08$. Combining the conclusions mentioned above, for symmetric nuclear matter, a dineutron BEC state will appear in the low-density limit for $\lambda \geqslant 1.10$ and there is only a weak coupling BCS state for $\lambda \lesssim 0.85$, which are similar as the pure neutron matter.

In Refs. [23,24], the BCS-BEC crossover is investigated by several characteristic quantities including the probability for the neutron pair partners $P(d_n)$ as well as the ratios ξ_{rms}/d_n, Δ_{Fn}/e_{Fn}, and ν_n/e_{Fn}, where Δ_{Fn} is the neutron pairing gap at the Fermi surface, e_{Fn} the neutron Fermi kinetic energy in Eq. (18) with $e_{Fn} = e(k = k_{Fn})$, ν_n the effective chemical potential, $P(d_n) = \int_0^{d_n} |\Psi_{pair}(r)|^2 r^2 dr$ with the average interneutron distance $d_n \equiv \rho_n^{-1/3}$ and $\Psi_{pair}(r)$ the neutron Cooper pair wave function in coordinate space, and the mean square radius of the neutron Cooper pairs $\xi_{rms}^2 = \int |\Psi_{pair}(r)|^2 r^4 dr / \int |\Psi_{pair}(r)|^2 r^2 dr$. As these characteristic quantities are monotonic functions of the dimensionless parameter $1/(k_{Fn}a)$ in the regularized gap equation approach [23,43,44], they can be used to describe the boundaries of BCS-BEC crossover.

In Table II are respectively listed the values of $P(d_n)$, ξ_{rms}/d_n, Δ_{Fn}/e_{Fn}, and ν_n/e_{Fn} characterizing the BCS-BEC crossover in the pure neutron matter for the dimensionless parameter $1/(k_{Fn}a) = 0, \pm1$, the zero-momentum transfer

density correlation function $D(0) = 0$, and the effective chemical potential $\nu_n = 0$ with effective pairing factors $\lambda = 1.0, 1.1, 1.2$. The corresponding values for symmetric nuclear matter are given in the parentheses. For comparison, the values in the regularized contact interaction model [23,43] are also given.

In Table II, it is shown that the values of $P(d_n)$, ξ_{rms}/d_n, and ν_n/e_{Fn} are almost independent of the pairing interaction strength and are similar for the pure neutron matter and the symmetric nuclear matter. Furthermore, the values of $P(d_n)$, ξ_{rms}/d_n, and ν_n/e_{Fn} are consistent with the results obtained in the regularized contact interaction model [23,43]. In Table II, the values of Δ_{Fn}/e_{Fn} slightly increase with the pairing interaction strength, which might be ascribed to the fact that the pairing gap Δ_{Fn} increases with the pairing force strength faster than the neutron Fermi kinetic energy e_{Fn} does. Furthermore, difference between the present Δ_{Fn}/e_{Fn} and those in the regularized contact interaction model [23] exists, which might be ascribed to the pairing force, i.e., the Bonn potential here and the constant interaction in the regularized contact interaction model. As the reference values of the characteristic quantities $P(d_n)$, ξ_{rms}/d_n, Δ_{Fn}/e_{Fn}, and ν_n/e_{Fn} characterizing the boundaries of BCS-BEC crossover are obtained in the relativistic framework by a self-consistent way and are consistent with those got by the regularized contact interaction model of nonrelativistic framework in Refs. [23,43], they provide a valuable guide in characterizing BCS-BEC crossover boundaries in future investigations.

IV. CONCLUSION

In conclusion, the influence of the pairing interaction strength on the dineutron correlations in the $^1S_0$ channel and the

BCS-BEC crossover phenomenon in nuclear matter has been investigated based on the RHB theory. The effective interaction PK1 is adopted in the ph channel and the Bonn-B potential is used in the pp channel. The influence of medium polarization effects on the pairing properties and the possible ambiguity of pairing force are simulated by an effective factor λ appending on the Bonn-B potential.

From the dimensionless parameter $1/(k_{Fn}a)$, the zero-momentum transfer density correlation function $D(0)$ and the effective chemical potential ν_n, a dineutron BEC state will occur at dilute density if $\lambda \geqslant 1.10$, and there is only a BCS state if $\lambda \lesssim 0.85$. Moreover, the reference values of several characterized quantities $P(d_n)$, ξ_{rms}/d_n, Δ_{Fn}/e_{Fn}, and ν_n/e_{Fn} characterizing the boundaries of BCS-BEC crossover are obtained in the self-consistent relativistic framework and are consistent with the nonrelativistic results [23,43], which may provide a valuable guide in characterizing BCS-BEC crossover boundaries in future investigations.

[1] D. M. Eagles, Phys. Rev. **186**, 456 (1969).

[2] A. J. Leggett, J. Phys. Colloq. **41**, 7 (1980).

[3] P. Nozières and S. Schmitt-Rink, J. Low Temp. Phys. **59**, 195 (1985).

[4] Y. Ohashi and A. Griffin, Phys. Rev. Lett. **89**, 130402 (2002).

[5] M. Greiner, C. A. Regal, and D. S. Jin, Nature (London) **426**, 537 (2003).

[6] S. Jochim, M. Bartenstein, A. Altmeyer, G. Hendl, S. Riedl, C. Chin, J. H. Denschlag, and R. Grimm, Science **302**, 2101 (2003).

[7] M. W. Zwierlein, C. A. Stan, C. H. Schunck, S. M. F. Raupach, S. Gupta, Z. Hadzibabic, and W. Ketterle, Phys. Rev. Lett. **91**, 250401 (2003).

[8] T. Alm, B. L. Friman, G. Röpke, and H. Schulz, Nucl. Phys. A **551**, 45 (1993).

[9] H. Stein, A. Schnell, T. Alm, and G. Röpke, Z. Phys. A **351**, 295 (1995).

[10] M. Baldo, U. Lombardo, and P. Schuck, Phys. Rev. C **52**, 975 (1995).

[11] U. Lombardo and P. Schuck, Phys. Rev. C **63**, 038201 (2001).

[12] A. Sedrakian and J. W. Clark, Phys. Rev. C **73**, 035803 (2006).

[13] M. Jin, M. Urban, and P. Schuck, Phys. Rev. C **82**, 024911 (2010).

[14] G. F. de Téramond and B. Gabioud, Phys. Rev. C **36**, 691 (1987).

[15] M. Baldo, J. Cugnon, A. Lejeune, and U. Lombardo, Nucl. Phys. A **515**, 409 (1990).

[16] T. Takatsuka and R. Tamagaki, Prog. Theor. Phys. Suppl. **112**, 27 (1993).

[17] D. J. Dean and M. Hjorth-Jensen, Rev. Mod. Phys. **75**, 607 (2003).

[18] W. von Oertzen and A. Vitturi, Rep. Prog. Phys. **64**, 1247 (2001).

[19] J. Meng and P. Ring, Phys. Rev. Lett. **77**, 3963 (1996).

[20] J. Meng, Nucl. Phys. A **635**, 3 (1998).

[21] J. Meng, Phys. Rev. C **57**, 1229 (1998).

[22] A. Spyrou *et al.*, Phys. Rev. Lett. **108**, 102501 (2012).

[23] M. Matsuo, Phys. Rev. C **73**, 044309 (2006).

[24] J. Margueron, H. Sagawa, and K. Hagino, Phys. Rev. C **76**, 064316 (2007).

[25] A. A. Isayev, Phys. Rev. C **78**, 014306 (2008).

[26] S. J. Mao, X. G. Huang, and P. F. Zhuang, Phys. Rev. C **79**, 034304 (2009).

[27] B. Y. Sun, H. Toki, and J. Meng, Phys. Lett. B **683**, 134 (2010).

[28] Y. Kanada-En'yo, N. Hinohara, T. Suhara, and P. Schuck, Phys. Rev. C **79**, 054305 (2009).

[29] X.-G. Huang, Phys. Rev. C **81**, 034007 (2010).

[30] K. Hagino, H. Sagawa, J. Carbonell, and P. Schuck, Phys. Rev. Lett. **99**, 022506 (2007).

[31] H. Kucharek and P. Ring, Z. Phys. A **339**, 23 (1991).

[32] F. Matera, G. Fabbri, and A. Dellafiore, Phys. Rev. C **56**, 228 (1997).

[33] J. Li, B. Y. Sun, and J. Meng, Int. J. Mod. Phys. E **17**, 1441 (2008).

[34] L. G. Cao, U. Lombardo, and P. Schuck, Phys. Rev. C **74**, 064301 (2006).

[35] B. D. Serot and J. D. Walecka, Adv. Nucl. Phys. **16**, 1 (1986).

[36] P. Ring, Prog. Part. Nucl. Phys. **37**, 193 (1996).

[37] J. Meng, H. Toki, S. G. Zhou, S. Q. Zhang, W. H. Long, and L. S. Geng, Prog. Part. Nucl. Phys. **57**, 470 (2006).

[38] R. Machleidt, Adv. Nucl. Phys. **19**, 189 (1989).

[39] J. Bardeen, L. N. Cooper, and J. R. Schrieffer, Phys. Rev. **108**, 1175 (1957).

[40] R. Machleidt, *Computional Nuclear Physics 2 - Nuclear Reactions* (Springer, New York, 1993), p. 1.

[41] W. Long, J. Meng, N. VanGiai, and S.-G. Zhou, Phys. Rev. C **69**, 034319 (2004).

[42] C. A. R. Sáde Melo, M. Randeria, and J. R. Engelbrecht, Phys. Rev. Lett. **71**, 3202 (1993).

[43] J. R. Engelbrecht, M. Randeria, and C. A. R. Sáde Melo, Phys. Rev. B **55**, 15153 (1997).

[44] M. Marini, F. Pistolesi, and G. C. Strinati, Eur. Phys. J. B **1**, 151 (1998).

[45] M. Randeria, *Bose-Einstein Condensation* (Cambridge University Press, Cambridge, UK, 1995).

[46] B. Mihaila, S. Gaudio, K. B. Blagoev, A. V. Balatsky, P. B. Littlewood, and D. L. Smith, Phys. Rev. Lett. **95**, 090402 (2005).